International Immunopharmacology 75 (2019) 105826

Contents lists available at ScienceDirect

International Immunopharmacology

journal homepage: www.elsevier.com/locate/intimp

LDC000067 suppresses RANKL-induced osteoclastogenesis in vitro and prevents LPS-induced osteolysis in vivo

Song Xue[a,b,1], Qing Shao[a,1], Li-Bo Zhu[a], Ya-Fei Jiang[a,b], Cong Wang[a], Bao Xue[a], Hai-Ming Lu[a], Wei-Lin Sang[a,*], Jin-Zhong Ma[a,*]

[a] Department of Orthopedics, Shanghai General Hospital, Shanghai Jiao Tong University School of Medicine, Shanghai, 200080, China
[b] Shanghai Bone Tumor Institution, Shanghai, 201620, China

ARTICLE INFO

Keywords:
CDK9
LDC000067
Osteoclast
NF-κB
Osteolysis
Subchondral bone
LPS

ABSTRACT

Bone homeostasis requires a dynamic balance between osteogenesis and osteoclastogenesis, and osteolytic disorders are mainly attributed to aberrant osteoclastogenesis and bone resorption. Accumulating evidence has demonstrated that cyclin-dependent kinase 9 (CDK9) regulates some inflammatory diseases without affecting the cell cycle. Whether the specific inhibitor of CDK9, LDC000067 (abbreviated as LDC067), helps to prevent from osteolytic disorders has not been fully elucidated. Interestingly, this study demonstrated that LDC067 inhibited receptor activator of nuclear factor-κB ligand (RANKL)-induced osteoclastogenesis and bone resorption in vitro, and suppressed the expression of osteoclast-related marker genes such as cathepsin K (CTSK), tartrate-resistant acid phosphatase (TRAP), dendrite cell-specific transmembrane protein (DC-STAMP), V-ATPase D2, calcitonin receptor (CTR) and nuclear factor of activated T cells cytoplasmic 1 (NFATc1). The bone protective effects of LDC067 can be partly explained by its suppression of nuclear factor-kappa B (NF-κB)-mediated NFATc1 activation via AKT signalling pathway. In keeping with the results obtained in vitro, inhibition of CDK9 with LDC067 was observed to delay subchondral osteolysis and substantially ameliorate LPS-induced osteolysis in murine calvaria. Collectively, these results highlight the positive effects of LDC067 in preventing osteolytic disorders and indicate that this CDK9 inhibitor may a promising therapeutic agent.

1. Introduction

Bone homeostasis involves the dynamic balance between osteogenesis and osteoclastogenesis [1,2]. Given that over-activation of osteoclasts may disrupt the balance between bone formation activity and bone resorption activity, some osteolytic diseases may follow this over-activation, such as osteoporosis [3], Gorham-Stout syndrome [4] and rheumatoid arthritis [5]. Accumulating evidence has shown that one of the primary manifestations of osteoarthritis (OA) is lesions of the subchondral bone marrow; however, the articular cartilage is relatively intact [6,7]. Osteoclasts, as the only cells exerting bone resorption activity in bone tissue [8], are closely related to the bone resorption-related diseases mentioned above; therefore, these cells may be targets for the treatment or prevention of osteolytic disease.

RANKL, generated and released by osteoblasts and osteocytes, could bind to RANK receptors on pre-osteoclasts or mature osteoclasts [9] and could subsequently activate intracellular signalling cascades, such as AKT [10], NF-κB [11] and mitogen-activated protein kinases (MAPKs) [12,13], thereby inducing the activation of some crucial downstream regulatory factors, such as cellular oncogene fos (c-Fos) and NFATc1 [14], which could bind to the promoters of some marker genes of osteoclasts, such as CTSK, TRAP, DC-STAMP and CTR [15].

Currently, increasing numbers of compounds have been investigated or developed to cure some osteolytic diseases; these compounds include calcitonin [16], cathepsin-K inhibitor [17], bisphosphonates [18] and some traditional Chinese herbs [19]. However, discovering more drugs that target osteoclasts with better efficacy and fewer side effects is of great importance for clinical therapy.

Numerous studies have confirmed that CDK9 is associated with many inflammatory diseases [20–22]. This association may be attributed to the ability of CDK9 to rapidly recruit to the transcription complex and subsequently phosphorylate RNA polymerase II (Pol II) upon inflammatory

Abbreviations: CDK9, cyclin-dependent kinase 9; OA, osteoarthritis; LDC067, LDC000067; BMMs, bone marrow macrophages; RANKL, receptor activator of nuclear factor-κB ligand; NFATc1, nuclear factor of activated T cells cytoplasmic 1; NF-κB, nuclear factor-kappa B; ACLT, anterior cruciate ligament transection

* Corresponding authors.
E-mail addresses: sang_weilin@163.com (W.-L. Sang), majinzhong1963@sina.com (J.-Z. Ma).
[1] These authors contributed equally to this work.

https://doi.org/10.1016/j.intimp.2019.105826
Received 14 June 2019; Received in revised form 11 August 2019; Accepted 12 August 2019
Available online 19 August 2019

stimulation, which helps the Pol II to escape promoter pausing. Therefore, the transcriptional process is continuous [23]. However, the potential role of CDK9 in the development of osteolysis diseases warrants further investigation. The specific inhibitor of CDK9, LDC067, has recently been found to have many pharmacological effects [24], including anti-tumor and anti-inflammatory effects. However, to the best of our knowledge, the potential function of LDCC067 in osteolytic diseases has not been determined to date. In our research, we investigated the effects of LDC067 on osteolysis-related diseases and demonstrated the related mechanism governing these effects.

2. Materials and methods

2.1. Materials

LDC000067, purchased from Selleck Chemicals (Houston, TX, USA), was dissolved in DMSO (Sigma, St. Louis, MO, USA). Cell culture reagents and lipopolysaccharides (LPS) were purchased from Thermo Fisher Scientific (Scoresby, Victoria, Australia). Tartrate-resistant acid phosphatase (TRAP) staining kit and foetal bovine serum (FBS) were obtained from Sigma Aldrich (St. Louis, MO, USA). All cytokines, such as RANKL and macrophage colony stimulating factor (M-CSF), were purchased from R&D Systems (Minneapolis, MN, USA). Anti-CDK9, anti-p65, anti-p-p65, anti-IκBα, anti-ERK, anti-p-ERK, anti-JNK, anti-p-JNK, anti-p38, anti-p-p38, anti-AKT, anti-p-AKT, anti-Bcl-2, anti-Bax, anti-Bcl-xl, anti-C-PARP and anti-PARP antibodies were purchased from Cell Signaling Technology (Beverly, MA, USA). Antibodies against NFATc1 and c-Fos were purchased from Abcam (Hong Kong, China). All loading control antibodies, including GAPDH, β-actin and β-tubulin, were all purchased from Santa Cruz Biotechnologies (CA, USA).

2.2. Bone marrow macrophage (BMM) isolation and culture

C57BL/6 mice aged four weeks were sacrificed. Their bilateral femurs and tibia were transferred to the ultra-clean table, and we then carefully separated the surrounding muscles and connective tissue. After removing the tibia and femur of the mouse, we rinsed the bone using PBS three times for 1 min per time, and then disconnected the ends of the long bones with sterile scissors. To ensure that the cells flushed into the α-MEM containing 10 ng/mL M-CSF, we rinsed the bone marrow with a 1 ml syringe needle three times. At nearly 90% confluence, cells were digested with trypsin for 20 min to ensure that almost all the cells were harvested.

2.3. Cell viability

Cell Counting Kit-8 (CCK-8) (Dojindo, Japan) was used to assess the effect of LDC067 on cell viability according to the manufacturer's instructions. First, BMMs (8×10^3 cells per well) were pretreated with different concentrations of LDC000067 for several different times and then incubated with 10% CCK-8 working solution at 37 °C for 2 h. Optical density was measured by a microplate spectrophotometer (Spectra Max; Molecular Devices, Sunnyvale, USA) at a wavelength of 450 nm. All experiments were performed three times independently.

2.4. Quantitative reverse transcription polymerase chain reaction (qRT-PCR)

After treatment, total RNA was extracted from BMMs using TRIzol (TRI reagent) (Invitrogen, CA, USA). These RNA samples were transcribed into cDNA by M-MLV reverse transcriptase (Invitrogen, CA, USA). The relative expression of various target genes was determined by RT-PCR using SYBR® Premix Dimer Eraser TM (Perfect Real Time, TaKaRa, Japan) as previously reported [25]. β-actin was considered a housekeeping gene. The primer sequences are shown specifically in Table S1.

2.5. Flow cytometric analysis

BMMs were seeded in 6-well plates at a density of 5×10^5 cells/well and treated with gradient concentrations of LDC067 (0, 0.25, 0.5, 1, 2 and 4 μM/L) for 48 h. After the indicated time, the cells were all collected, washed with PBS, and resuspended in 1 × binding buffer containing Annexin V-FITC and PI. After incubation for 15 min at room temperature in the dark, the cells were analyzed via flow cytometry (BD Biosciences).

2.6. Immunoblotting

Immunoblotting was performed according to our previous report [25]. In short, ice-cold radioimmunoprecipitation (RIPA) containing protease and phosphatase inhibitors (Sigma, St. Louis, MO, USA) was used to lyse cells for 30 min. A pierce BCA protein assay kit (Beyotime, Nanjing, China) was used to quantify the collected proteins. Proteins were separated by SDS-PAGE electrophoresis and then transferred to polyvinylidene difluoride (PVDF) membranes (Millipore, Billerica, MA, USA). The PVDF membranes were blocked with 5% (*w/v*) nonfat milk for 60 min and incubated overnight at 4 °C with specific primary antibodies. After washed 3 times with PBST (10 min per time), the membranes were incubated for 60 min with peroxidase-conjugated secondary antibody (1:5000 dilution) (Sigma, St. Louis, MO, USA). After washed with PBST again for three times (10 min per time), signal bands were finally detected with an enhanced chemiluminescence reagent (Millipore, Billerica, MA, USA).

2.7. Osteoclast differentiation assay

Cell culture complete medium supplemented with M-CSF (30 ng/mL) and RANKL (50 ng/mL) was used to induce osteoclast differentiation in vitro. First, BMMs were seeded in 96-well plates in triplicate and cultured for 24 h. The number of cells per well was 8×10^3 cells per well. Various concentrations of LDC067 (0, 1, 2, and 4 μM/L) were then added to osteoclast differentiation medium, and the medium was changed every two days. After incubation for seven days, the differentiation process stopped, and all the cells were fixed with 4% paraformaldehyde (PFA) for 15 to 20 min. Afterwards, the cells were stained with a TRAP staining kit and rhodamine-conjugated phalloidin (Cytoskeleton, Denver, USA). The number of TRAP (+) cells (with more than three nuclei) were counted per well.

2.8. Osteoblast differentiation analysis

Ascorbic acid (50 μM/L), β-glycerophosphate (10 mmol/L) and dexamethasone (100 nM/L) were added to complete medium as osteogenic induction medium. BMSCs were treated with this medium for 14 days and then stained with Alizarin Red according to a previous report [26].

2.9. Nuclear and cytoplasmic extraction

To detect the expression of some proteins from the nucleus and cytoplasm, a nuclear extraction kit (Beyotime, Jiangsu, China) was used according to our previous report [25]. After the proteins were collected, we used western blotting to uncover the expression of p65 in the nucleus and cytoplasm.

2.10. Immunofluorescence microscopy

First, after fixation with 4% PFA for 15 min, BMMs were permeabilized with 0.1% Triton X-100 for 5 min. Afterwards, the BMMs were blocked with 3% BSA for half an hour and then incubated with antibody against p65 (1:400) overnight at 4 °C. TBST solution was used to wash the cells extensively (three times, 5 min per time). We used Alexa Fluor

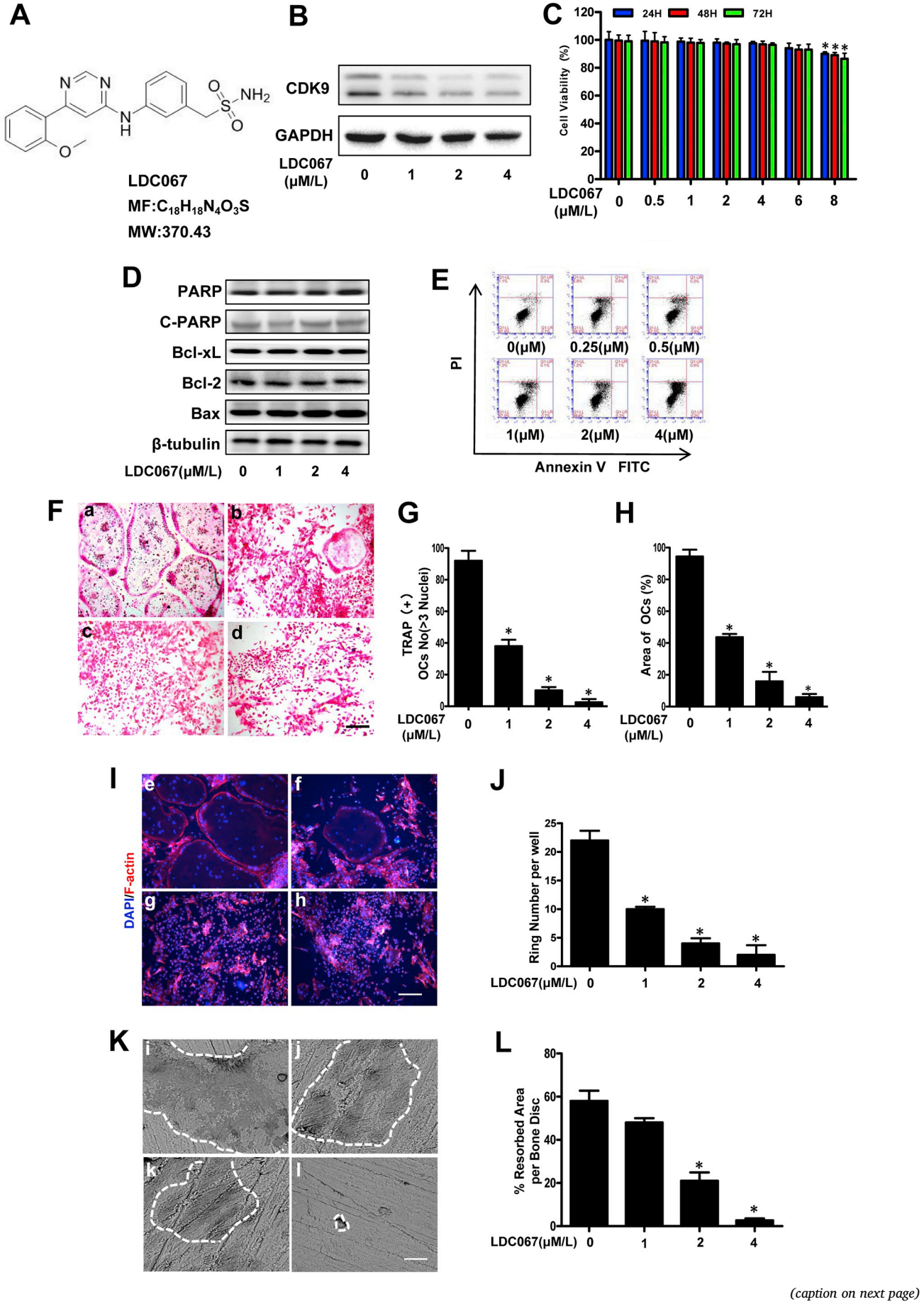

(caption on next page)

Fig. 1. LDC067 prevents osteoclastogenesis and bone resorption in vitro. (A) The chemical structure of LDC067 is presented. (B) LDC067 could surely inhibited CDK9 in BMMs in a concentration-dependent manner. (C) The effect of LDC067 on the cell viability of mouse BMMs was measured by CCK-8. (D) Expression of proteins involved in the intrinsic caspase cascade was assessed using western blotting, β-tubulin served as a loading control. (E) BMMs treated with a range of concentrations of LDC067 for 48 h were stained with Annexin V-FITC and PI to determine the percentage of dead and apoptotic cells within each population. (F) The effect of LDC067 on BMM differentiation was detected using TRAP staining (a-d, treated with LDC067 at 0, 1, 2, and 4 μM/L, respectively). Scale bar, 100 μm. (G, H) The number of TRAP-positive osteoclasts (≥3 nuclei) and the area of osteoclasts per well were quantified. (I) Osteoclasts were treated with M-CSF (30 ng/ml), RANKL (50 ng/ml) and a range of concentrations of LDC067 for seven days, stained with F-actin and then examined by immunofluorescence microscopy (e-h, treated with LDC067 at 0, 1, 2, and 4 μM/L, respectively). Scale bar, 100 μm. (J) The number of osteoclasts with an intact actin ring was quantified. (K) Bone resorption pits were observed by scanning electron microscopy. Scale bar, 200 μm. (L) The resorbed area on each bone disc was quantified by a SEM and expressed as a percentage of the total bone disc area (i–l, treated with LDC067 at 0, 1, 2 and 4 μM/L, respectively). All bar graphs are expressed as the mean ± SD. The data presented are representative of at least three independent experiments. *P < 0.05 compared to the control.

488-conjugated secondary antibodies for further detection. Cells were incubated with DAPI for 10 min to stain cell nuclei. Then, the cells were washed with PBST for 3 times (5 min per time). Finally, a Leica confocal fluorescence microscope was used to collect images.

2.11. Bone resorption pit assay

Equal numbers of osteoclasts were seeded onto bovine bone discs (5 mm × 5 mm) (Corning, NY, USA) in 96-well plates in triplicate and incubated with different concentrations of LDC067 (0, 1, 2 and 4 μM/L) for two days. Bone discs were then gently brushed with 2 M NaOH to remove the attached cells. Then the bone discs were detected with a scanning electron microscope (SEM) (Philips XL30) and the percentage of bone resorption area was further calculated by ImageJ software (NIH, Bethesda, MD, USA).

2.12. Experimental ACLT mouse model establishment and treatment

Our animal experiments were approved by the Animal Experimental Center of Shanghai General Hospital (Number: 2018KY201). Twenty male C57BL/6 mice aged 4 weeks were raised at the animal care centre. According to our previous report [27], anterior cruciate ligament transection (ACLT) was carried out to establish an experimental OA mouse model. In short, after anesthesia, a needle was inserted into the right knee cavity, and we ensured that the ACL was transected by the anterior drawer test. Mice were divided into four groups randomly and received different treatment for 6 weeks: mice from the sham group did not receive any injury; the other three groups all received ACLT surgery and intraperitoneal administration of PBS (7.5 mg/kg, 3 times a week), low-dose LDC067 (7.5 mg/kg, 3 times a week) and high-dose LDC067 (15 mg/kg, 3 times a week). The body weight of mice was measured at different lengths of time after administration.

2.13. LPS-induced murine calvaria osteolysis model

Twenty male C57/BL6 mice aged 8 weeks were randomly divided into four treatment groups: (1) the sham group (PBS); (2) the LPS treatment group (5 mg/kg body weight); (3) LPS (5 mg/kg body weight) and LDC067 (7.5 mg/kg body weight); (4) LPS (5 mg/kg body weight) and LDC067 (15 mg/kg body weight). LPS were subcutaneously injected over the centre of the calvaria and administered every other day. Prophylactic treatment was performed one day before the LPS injection, and the PBS and LPS + LDC067 groups were injected with corresponding doses of PBS or LDC067. Fourteen days after the first LPS injections, mice were all sacrificed. Afterwards, all the calvarial samples were collected and fixed in 4% PFA for further experiments.

2.14. Micro-CT analysis

After treatment, the calvaria and right femur bone were harvested and fixed in 4% formaldehyde for 1 day. Afterwards, a high-resolution micro-CT was conducted for three-dimensional (3D) histomorphometric analysis with the assistance of YueBo Corporation. The isotropic resolution was 6 μm and the 3D images showed the detailed structure of subchondral trabecula bone and calvaria bone. Several bone-related parameters, including bone volume/total tissue volume (BV/TV), trabecular number (Tb. N.), trabecular separation (Tb. Sp.) and trabecular thickness (Tb. Th.), were included in our 3D structural analysis.

2.15. Histopathology and immunohistochemistry

After decalcification for 2 weeks, all the samples were collected and embedded in paraffin and sectioned with a microtome (4-μm-thick sections). These sections were stained with TRAP to quantify the numbers of osteoclasts with ImageJ software. For immunohistochemistry analysis, these sections were stained with primary antibodies according to our previous research [26].

2.16. Statistical analysis

All data were presented as the mean ± SD with $N \geq 3$. To compare the differences between two groups and among three or more groups, student's *t*-test and one-way ANOVA were performed, respectively. Statistical significance was indicated by *p*-values < 0.05.

3. Results

3.1. LDC067 prevents RANKL-induced osteoclastogenesis and impairs osteoclast-mediated bone resorption in vitro

The effectiveness of LDC067 was firstly assessed. As shown in Fig. 1B, LDC067 suppressed CDK9 expression in a concentration-dependent manner. An in vitro CCK-8 assay was carried out to identify the concentration of LDC067 that inhibited BMM proliferation and survival. Our results showed that up to 6 μM/L LDC067 had no significant anti-proliferation and cytotoxic effects on BMMs compared with the control (Fig. 1C). The expression levels of proteins involved in the intrinsic caspase cascade were assessed; however, there were no obvious changes regarding the expression of apoptosis-related proteins, including Bax, Bcl-2 and Bcl-xL, or the activation of the PARP apoptotic pathway (Fig. 1D). Furthermore, BMMs were treated with various concentrations of LDC067 ranging from 0 to 4 μM/L for 2 days and then stained with Annexin V-FITC and PI to detect the percentage of apoptotic or necrotic cells. Until the concentration was up to 4 μM/L, LDC067 did not significantly influence the in vitro cell apoptosis rates (Fig. 1E). Because BMMs are osteoclast progenitors, the effect of LDC067 on RANKL-induced osteoclastogenesis was further investigated. As a result, we found that LDC067 could significantly inhibit the formation of TRAP (+) osteoclasts in a concentration-dependent manner (Fig. 1F-H). Moreover, LDC067 dose-dependently reduced the number of F-actin rings, which were considered as the marker of fusion and maturation of osteoclast progenitors (Fig. 1I and J). We further explored the effects of LDC067 on the function of osteoclasts by performing a bone pit resorption assay in vitro. Mature osteoclasts were seeded onto bovine bone slices and stimulated with a range of concentrations of LDC067 (0, 1, 2 and 4 μM/L) for 48 h, and then the bovine bone slices were examined by SEM. As expected, the areas of bone

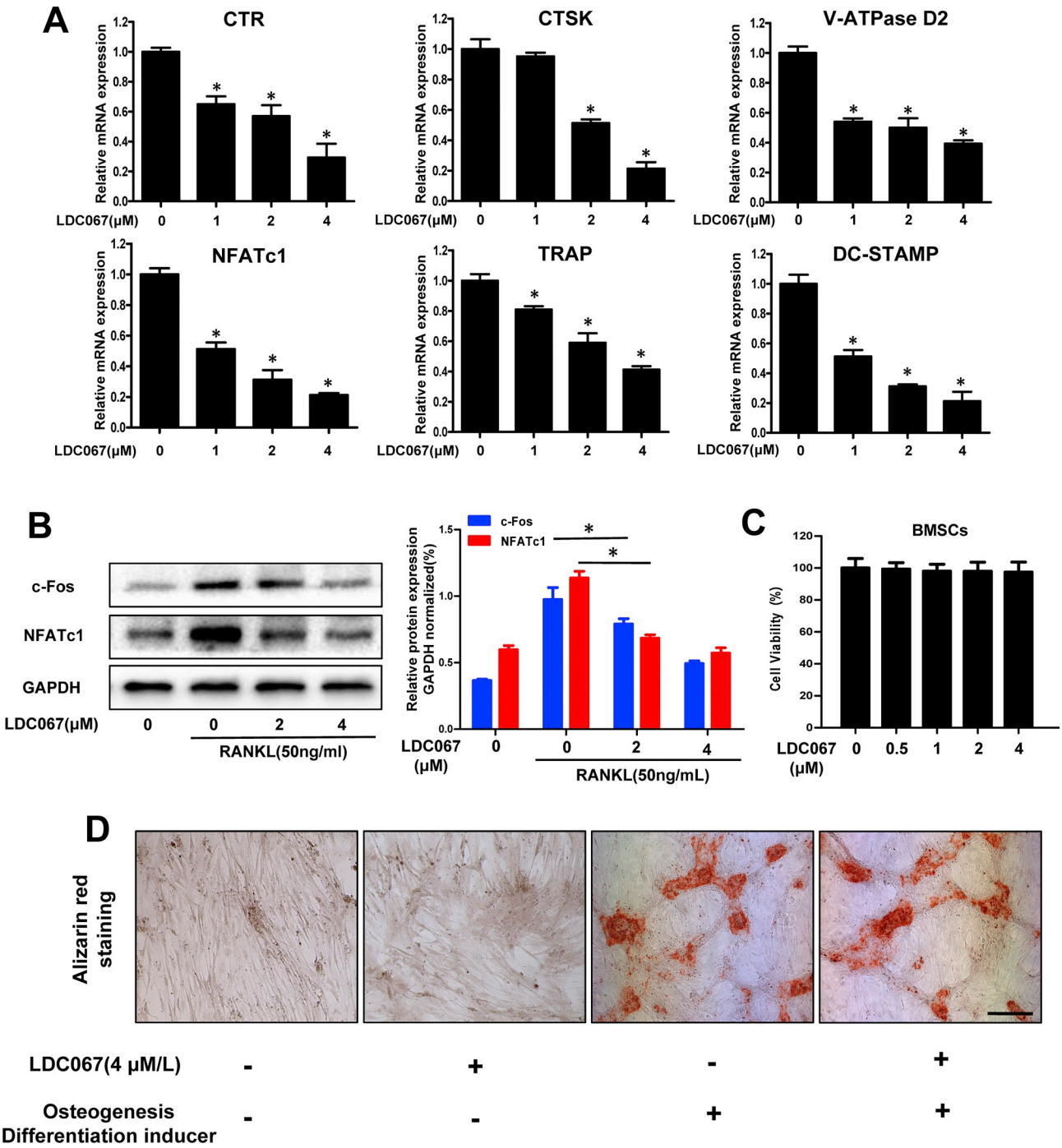

Fig. 2. LDC067 dose-dependently suppresses the expression of osteoclast marker genes. (A) The expression of osteoclast marker genes (DC-STAMP, CTSK, CTR, TRAP, V-ATPase D2 and NFATc1) was determined using RT-qPCR. The gene expression of target genes was normalized to that of β-actin. (B) LDC067 suppressed the RANKL-induced (50 ng/ml) activation of c-Fos and NFATc1. GAPDH was used as the loading control. The protein expression levels of c-Fos and NFATc1 were quantified using ImageJ (right panel). (C) The effect of LDC067 on the cell viability of BMSCs after 72 h treatment was measured via CCK-8 assay. (D) The effects of LDC067 on osteogenesis were detected using Alizarin Red staining. Scale bar, 200 μm. Data are shown as the mean ± SD of triplicate independent experiments. *P < 0.05 vs the control group, n = 3.

resorption (Fig. 1K and L) gradually decreased. Collectively, these data demonstrated that LDC067 suppressed osteoclast-mediated bone resorption activity in vitro.

3.2. LDC067 suppresses bone resorption-related gene expression in a dose-dependent manner

As shown in Fig. 2A, we revealed that LDC067 downregulated some osteoclast marker genes expression, including DC-STAMP, CTSK, NFATc1, TRAP, CTR and V-ATPase D2, by day 5 via qRT-PCR and clarified the mechanism of LDC067 on osteoclastogenesis. Given that c-Fos and NFATc1 play significant roles in osteoclastogenesis and inducing the expression of some bone resorption-related genes, we subsequently determined whether LDC067 affected the c-Fos/NFATc1 signalling pathway. Interestingly, after treatment with RANKL (50 ng/mL) for 72 h, the expression of c-Fos and NFATc1 were all significantly

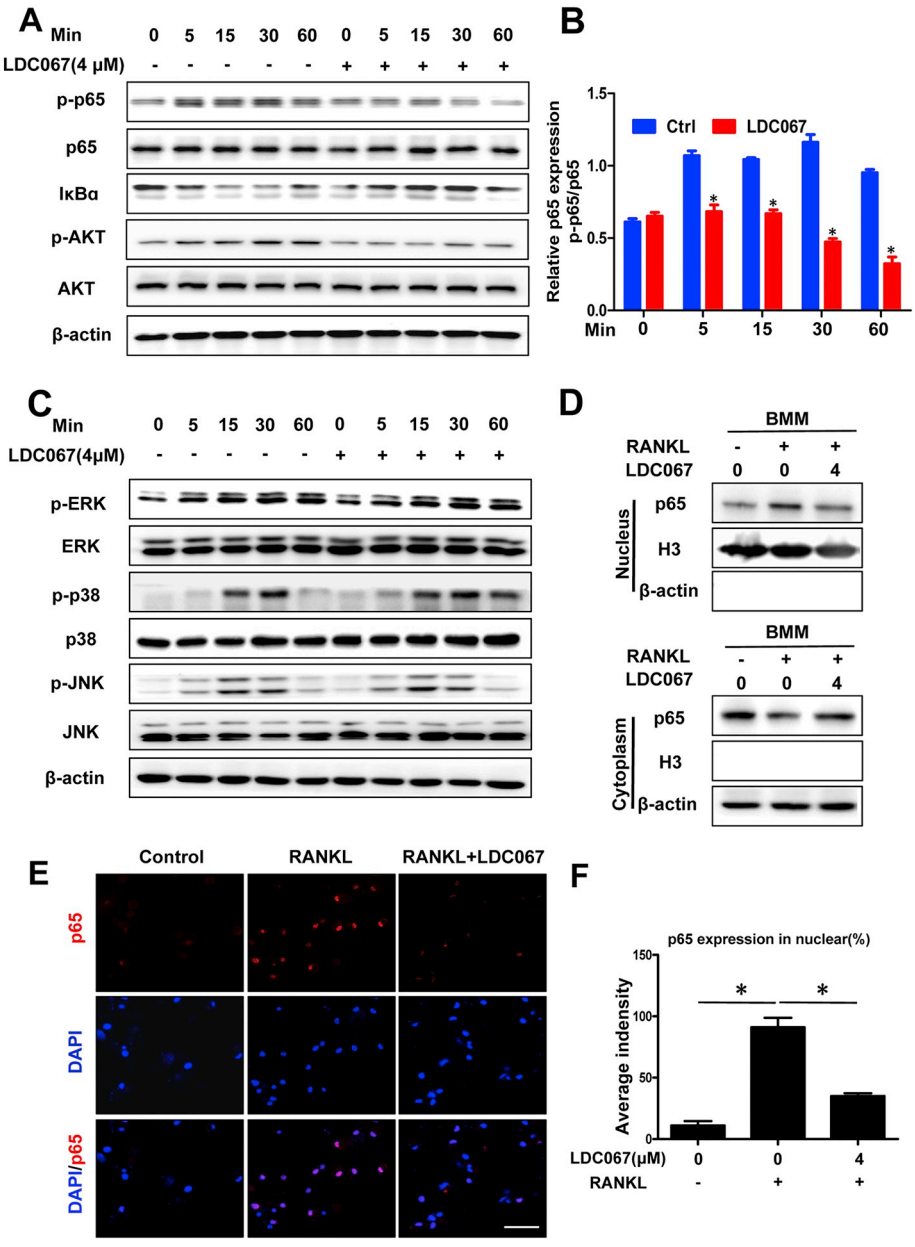

Fig. 3. LDC067 attenuates the activation of the AKT/NF-κB signalling pathways in BMMs. (A) The activity of the AKT/NF-κB signalling pathways in BMMs was evaluated by western blotting. β-actin was used as a loading control. (B) The ratio of p-p65 to total p65 was quantified using ImageJ. (C) The activity of the MAPK signalling pathway in BMMs was evaluated by western blotting and β-actin was used as a loading control. (D) The expression and nuclear translocation of NF-κB p65 in BMMs were determined by nuclear-cytoplasmic extraction assay. (E) Immunofluorescence was also performed to determine the expression and nuclear translocation of NF-κB p65 in BMMs. (F) Quantitative analysis of p65 in the nuclei of BMMs via calculating average intensity. The data presented are representative of at least 3 independent experiments. All bar graphs present the mean ± SD. *P < 0.05 compared with the control group.

increased, while LDC067 suppressed this effect in a concentration-dependent manner (Fig. 2B).

Since bone homeostasis requires a dynamic balance between osteogenesis and osteoclastogenesis, the effect of LDC067 on osteogenesis was also investigated. First, as shown in Fig. 2C, until the concentration was up to 4 μM/L, LDC067 did not have significant cytotoxic effects on BMSCs. The experiment of osteoblast differentiation from progenitors with or without LDC067 was performed. After 14 days of induction with differentiation inducer, osteogenic differentiation was determined by Alizarin Red staining; however, the results showed that there was no significant difference between the two groups (Fig. 2D), that is, LDC067 had no significant effect on osteogenesis.

3.3. LDC067 attenuates the activation of the AKT/NF-κB signalling pathways

The AKT, NF-κB and MAPK signalling pathways are key signalling transduction pathways that are involved in RANKL-induced osteoclastogenesis. Therefore, we further investigated these signalling pathways to illuminate the related mechanisms of LDC067 in preventing osteoclastogenesis and osteolysis. The total and phosphorylation status of the key signalling proteins in these pathways were detected via western blotting. As shown in Fig. 3A and B, RANKL treatment induced phosphorylation of p65 and AKT, however, LDC067 treatment rescued this effect. The ratio of the intensity of p-p65 to p65 was significantly lower in the LDC067 treatment group than in the no-LDC067 treatment group at our indicated time points (5, 15, 30 and 60 min). However, LDC067 treatment did not have a significant effect on RANKL-induced phosphorylation of ERK, JNK and p38 (Fig. 3C). Importantly, these data suggest LDC067's inhibitory effects on osteoclastogenesis and osteolysis in vitro, possibly due to inhibition of the AKT/NF-κB signalling pathway activation. Furthermore, a nuclear-cytoplasmic extraction assay and immunofluorescence analysis were performed, and all the results showed that RANKL-induced p65 nuclear translocation in BMMs, while this CDK9 inhibitor repressed the effect (Fig. 3D–F). Collectively, these results demonstrated that LDC067 treatment blocked AKT/NF-κB signalling pathway activation.

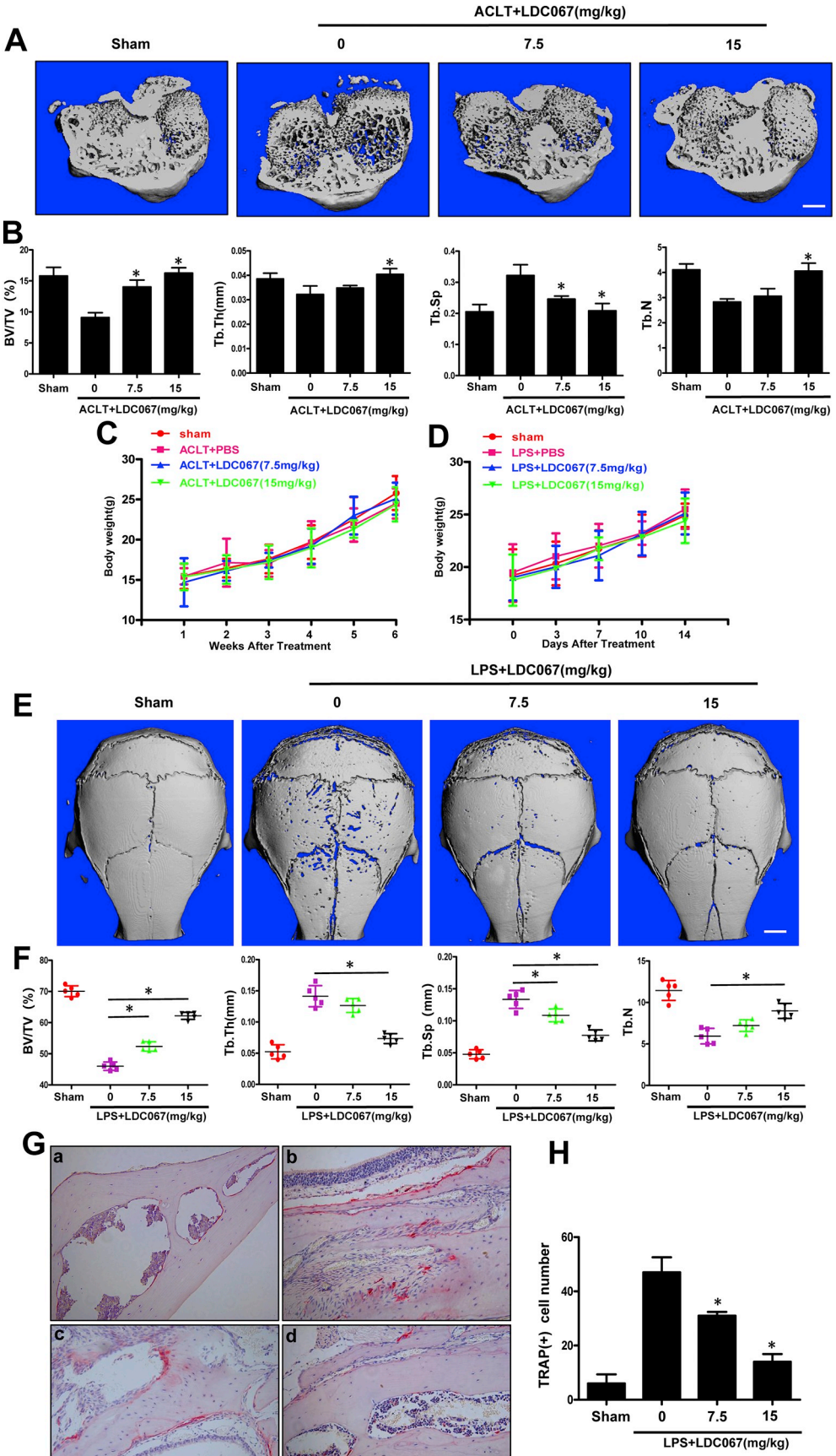

Fig. 4. LDC067 prevents bone resorption in the subchondral bone of OA and LPS-induced osteolysis. (A) Representative micro-CT 3D reconstructed images were obtained for the four groups. Scale bar, 1 mm. (B) The BV/TV, Tb. Th., Tb. N. and Tb. Sp. were measured. (C, D) The body weight changes after ACLT surgery and LPS treatment for the two groups, respectively. (E) Representative 3D reconstructed micro-CT images of the outside of the calvaria from the four groups two weeks after treatment. Scale bar, 1 mm. (F) The BV/TV, Tb. Th., Tb. N. and Tb. Sp. were measured. (G) TRAP staining of calvaria for the four groups, (a–d, representing the sham group, LPS + PBS treatment group, LPS + low-dose LDC067 treatment group and LPS + high-dose LDC067 treatment group, respectively) Scale bar, 100 μm. (H) Histomorphometric analysis of the number of TRAP (+) osteoclasts in the calvaria for the four groups. The data presented are representative of at least 3 independent experiments. All bar graphs present the mean ± SD; *P < 0.05 compared with the control.

3.4. LDC067 effectively prevents bone resorption both in the ACLT-induced subchondral osteolysis and acute LPS-induced osteolysis model

Six weeks after surgery, mice from four groups were sacrificed and the right femur bone was harvested. We used micro-CT 3D reconstructed images to show the bone resorption degree. As shown in Fig. 4A, the subchondral bone of the mice from ACLT group exhibited extensive dissolution. However, intraperitoneal injections of LDC067 in the ACLT mouse model dramatically attenuated the loss of tibial subchondral bone in a dose-dependent manner. Some bone parameters, such as BV/TV (%), Tb. Th., Tb. N. and Tb. Sp., were also measured (Fig. 4B). We measured the mice body weight after ACLT surgery per week (Fig. 4C). After determining that LDC067 exhibited anti-osteoclastogenesis and antiresorptive capabilities, we further investigated the potential efficacy of LDC067 to prevent LPS-induced osteolysis of mice calvaria. The body weight changes of mice after LPS treatment were recorded for two weeks (Fig. 4D). Some bone parameters were also measured as previously reported [21], and the results indicated that prophylactic treatment with LDC067 could protect against LPS-induced osteolysis in vivo (Fig. 4E and F). In addition, TRAP staining was performed to show the osteoclast formation among the four groups. As demonstrated in Fig. 4G and H, the osteoclast formation was significant in the LPS-induced inflammatory osteolysis group compared with the sham group; while LDC067 treatment inhibited LPS-induced osteoclastogenesis in a dose-dependent manner in vivo.

4. Discussion

As previously reported, osteolytic bone diseases frequently occur when the balance between osteogenesis and osteoclastogenesis is disrupted. At present, it is now generally accepted that osteoclasts might be the target of some osteolytic diseases. In this study, we found that the CDK9 inhibitor LDC067 suppressed RANKL-induced osteoclastogenesis and bone resorption activities via inhibiting AKT/NF-κB and c-Fos/NFATc1 activation in vitro, and it delayed subchondral osteolysis in an ACLT mouse model. In addition, the effect of LDC067 on LPS-mediated osteolysis was investigated. We determined that LDC067 treatment could significantly protect against LPS-induced acute osteolysis, further broadening its application in bone tissue.

Osteoclasts are the cells that exert bone resorption activity and play significant roles in bone remodeling. Abnormal osteoclast activity could mediate the occurrence of various osteolytic diseases. The specific biological markers of bone resorption, including CTSK and TRAP, and the specific markers of osteoclast fusion, including DC-STAMP and V-ATPase D2, were repressed in a dose-dependent manner by LDC067. CDK9 was recently demonstrated to play an important role in various inflammatory diseases, such as titanium-induced osteolysis and post-traumatic osteoarthritis. In addition, some researchers revealed CDK9 inhibitor flavopiridol could exert protective effects on osteoporosis [28]. In this study, we found that LDC067 delayed subchondral osteolysis in the early stage of the mouse model.

To the best of our knowledge, M-CSF and RANKL, are the key cytokines for the fusion of preosteoclasts and the formation and maturation of osteoclasts [29]. RANKL binds to the RANK receptor on BMMs, facilitating pre-osteoclasts differentiation and maturation through the activation of AKT/NF-κB signalling pathway [30]. In this study, we demonstrated that LDC067 dose-dependently inhibited the activation of nuclear translocation of NF-κB p65, which are upstream of NFATc1. However, NFATc1, the key regulator of osteoclastogenesis, which is induced by c-Fos, could regulate osteoclast differentiation and maturation. Therefore, LDC067 could inhibit RANKL-induced c-Fos/NFATc1 expression and inhibit osteoclastogenesis in a concentration-dependent manner. LPS, from the cell wall of gram-negative bacteria [31], could stimulate the production of proinflammatory cytokines, such as TNF-α, IL-1β and IL-6, from the immune cells and subsequently promote the formation and maturation of osteoclasts, thereby leading to serious osteolysis [32,33]. In our study, we revealed that local injection of LPS increased the eroded surface area on mouse calvaria; however, pretreatment with LDC067 inhibited LPS-induced bone resorption, which might be correlated with LDC067-mediated inhibition of osteoclast differentiation and maturation.

In addition to NF-κB p65 and RANKL, CDK9 could regulate some other signalling pathways [34]. Therefore, there are other research directions that merit further investigation. Specifically, we performed two lytic bone disease mouse models and found that there are more osteolytic diseases that warrant further investigation, such as chronic osteoporosis, periodontitis and Gorham-Stout syndrome.

Taken together, this research revealed that CDK9 inhibition significantly suppressed osteoclastogenesis in vitro and could exert protective effects on both subchondral osteolysis and LPS-induced osteolysis in vivo. Our research provides strong evidence that LDC000067 may be a promising therapeutic agent against osteolytic disorders.

Supplementary data to this article can be found online at https://doi.org/10.1016/j.intimp.2019.105826.

Funding information

This work was greatly supported by the National Natural Science Foundation of China (NSFC) (NO. 81871795), Shanghai Hospital Development Center (No. SHDC12017121) and Songjiang District Science and Technology Project (No. 18sjkjgg18).

Declaration of competing interest

All authors declare there is no conflict of interest.

References

[1] X. Feng, J.M. McDonald, Disorders of bone remodeling, Annu. Rev. Pathol. 6 (2011) 121–145.
[2] S. Finzel, E. Sahinbegovic, R. Kocijan, K. Engelke, M. Englbrecht, G. Schett, Inflammatory bone spur formation in psoriatic arthritis is different from bone spur formation in hand osteoarthritis, Arthritis Rheum. 66 (11) (2014) 2968–2975 (Hoboken, N.J.).
[3] J.Y. Krzeszinski, W. Wei, H. Huynh, Z. Jin, X. Wang, T.C. Chang, X.J. Xie, L. He, L.S. Mangala, G. Lopez-Berestein, A.K. Sood, J.T. Mendell, Y. Wan, miR-34a blocks osteoporosis and bone metastasis by inhibiting osteoclastogenesis and Tgif2, Nature 512 (7515) (2014) 431–435, https://doi.org/10.1038/nature13375.
[4] S. Colucci, G. Taraboletti, L. Primo, A. Viale, C. Roca, D. Valdembri, M. Geuna, M. Pagano, M. Grano, A.M. Pogrel, A.L. Harris, N.N. Athanasou, A. Mantovani, A. Zallone, F. Bussolino, Gorham-Stout syndrome: a monocyte-mediated cytokine propelled disease, J. Bone Miner. Res. Off. J. Am. Soc. Bone Miner. Res. 21 (2) (2006) 207–218.
[5] J.H. Shim, Z. Stavre, E.M. Gravallese, Bone loss in rheumatoid arthritis: basic mechanisms and clinical implications, Calcif. Tissue Int. 102 (5) (2018) 533–546.
[6] D. Muratovic, D.M. Findlay, F.M. Cicuttini, A.E. Wluka, Y.R. Lee, J.S. Kuliwaba, Bone matrix mcrodamage and vascular changes characterize bone marrow lesions in the subchondral bone of knee osteoarthritis, Bone 108 (2018) 193–201.
[7] E. Kon, M. Ronga, G. Filardo, J. Farr, H. Madry, G. Milano, L. Andriolo, N. Shabshin, Bone marrow lesions and subchondral bone pathology of the knee, Knee Surg. Sports Traumatol. Arthrosc. 24 (6) (2016) 1797–1814.
[8] M. Mavragani, P. Brudvik, K.A. Selvig, Orthodontically induced root and alveolar bone resorption: inhibitory effect of systemic doxycycline administration in rats, Eur. J. Orthod. 27 (3) (2005) 215–225.
[9] J.M. Quinn, J. Elliott, M.T. Gillespie, T.J. Martin, A combination of osteoclast differentiation factor and macrophage-colony stimulating factor is sufficient for both human and mouse osteoclast formation in vitro, Endocrinology 139 (10) (1998) 4424–4427.
[10] L. Li, M. Sapkota, M. Gao, H. Choi, Y. Soh, Macrolactin F inhibits RANKL-mediated osteoclastogenesis by suppressing Akt, MAPK and NFATc1 pathways and promotes osteoblastogenesis through a BMP-2/smad/Akt/Runx2 signaling pathway, Eur. J. Pharmacol. 815 (2017) 202–209.
[11] Y.Q. He, Q. Zhang, Y. Shen, T. Han, Q.L. Zhang, J.H. Zhang, B. Lin, H.T. Song, H.Y. Hsu, L.P. Qin, H.L. Xin, Q.Y. Zhang, Rubiadin-1-methyl ether from Morinda officinalis how. Inhibits osteoclastogenesis through blocking RANKL-induced NF-kappaB pathway, Biochem. Biophys. Res. Commun. 506 (4) (2018) 927–931.
[12] J. Cao, Q. Lu, N. Liu, Y.X. Zhang, J. Wang, M. Zhang, H.B. Wang, W.C. Sun, Sciadopitysin suppresses RANKL-mediated osteoclastogenesis and prevents bone loss in LPS-treated mice, Int. Immunopharmacol. 49 (2017) 109–117.
[13] X. Yang, W. Gao, B. Wang, X. Wang, H. Guo, Y. Xiao, L. Kong, D. Hao, Picroside II inhibits RANKL-mediated osteoclastogenesis by attenuating the NF-kappaB and MAPKs signaling pathway in vitro and prevents bone loss in lipopolysaccharide

treatment mice, J. Cell. Biochem. 118 (12) (2017) 4479–4486.
[14] Y. Xiao, K. Li, Z. Wang, F. Fu, S. Shao, F. Song, J. Zhao, W. Chen, Q. Liu, J. Xu, Pectolinarigenin prevents bone loss in ovariectomized mice and inhibits RANKL-induced osteoclastogenesis via blocking activation of MAPK and NFATc1 signaling, J. Cell. Physiol. 234 (8) (2019) 13959–13968.
[15] X. Chen, X. Chen, Z. Zhou, A. Qin, Y. Wang, B. Fan, W. Xu, S. Zhang, LY411575, a potent gamma-secretase inhibitor, suppresses osteoclastogenesis in vitro and LPS-induced calvarial osteolysis in vivo, J. Cell. Physiol. 234 (11) (2019) 20944–20956, https://doi.org/10.1002/jcp.28699.
[16] J.C. Stevenson, I.M. Evans, Pharmacology and therapeutic use of calcitonin, Drugs 21 (4) (1981) 257–272.
[17] L.T. Duong, G.A. Wesolowski, P. Leung, R. Oballa, M. Pickarski, Efficacy of a cathepsin K inhibitor in a preclinical model for prevention and treatment of breast cancer bone metastasis, Mol. Cancer Ther. 13 (12) (2014) 2898–2909.
[18] R. F. Barghash, W. M. Abdou, Pathophysiology of metastatic bone disease and the role of the second generation of bisphosphonates: from basic science to medicine, Curr. Pharm. Des. 22 (11) (2016) 1546–1557.
[19] N.D. Zhang, T. Han, B.K. Huang, K. Rahman, Y.P. Jiang, H.T. Xu, L.P. Qin, H.L. Xin, Q.Y. Zhang, Y.M. Li, Traditional Chinese medicine formulas for the treatment of osteoporosis: implication for antiosteoporotic drug discovery, J. Ethnopharmacol. 189 (2016) 61–80.
[20] A. Hellvard, L. Zeitlmann, U. Heiser, A. Kehlen, A. Niestroj, H.U. Demuth, J. Koziel, N. Delaleu, P. Jan, P. Mydel, Inhibition of CDK9 as a therapeutic strategy for inflammatory arthritis, Sci. Rep. 6 (2016) 31441.
[21] U.K. Schmerwitz, G. Sass, A.G. Khandoga, J. Joore, B.A. Mayer, N. Berberich, F. Totzke, F. Krombach, G. Tiegs, S. Zahler, A.M. Vollmar, R. Furst, Flavopiridol protects against inflammation by attenuating leukocyte-endothelial interaction via inhibition of cyclin-dependent kinase 9, Arterioscler. Thromb. Vasc. Biol. 31 (2) (2011) 280–288.
[22] J.H. Yik, Z. Hu, R. Kumari, B.A. Christiansen, D.R. Haudenschild, Cyclin-dependent kinase 9 inhibition protects cartilage from the catabolic effects of proinflammatory cytokines, Arthritis Rheum. 66 (6) (2014) 1537–1546 (Hoboken, N.J.).
[23] S. Eyvazi, M.S. Hejazi, H. Kahroba, M. Abasi, R.E. Zamiri, V. Tarhriz, CDK9 as an appealing target for therapeutic interventions, Curr. Drug Targets 20 (4) (2019) 453–464.
[24] T.K. Albert, C. Rigault, J. Eickhoff, K. Baumgart, C. Antrecht, B. Klebl, G. Mittler, M. Meisterernst, Characterization of molecular and cellular functions of the cyclin-dependent kinase CDK9 using a novel specific inhibitor, Br. J. Pharmacol. 171 (1) (2014) 55–68.
[25] S. Xue, L. Zhu, C. Wang, Y. Jiang, H. Lu, Y. Liu, Q. Shao, B. Xue, W. Sang, J. Ma, CDK9 attenuation exerts protective effects on catabolism and hypertrophy in chondrocytes and ameliorates osteoarthritis development, Biochem. Biophys. Res. Commun. 517 (1) (2019) 132–139, https://doi.org/10.1016/j.bbrc.2019.07.032.
[26] Y. Jiang, W. Sang, C. Wang, H. Lu, T. Zhang, Z. Wang, Y. Liu, B. Xue, S. Xue, Z. Cai, Y. Hua, L. Zhu, J. Ma, Oxymatrine exerts protective effects on osteoarthritis via modulating chondrocyte homoeostasis and suppressing osteoclastogenesis, J. Cell. Mol. Med. 22 (2018) 3941–3954, https://doi.org/10.1111/jcmm.13674.
[27] Y. Jiang, L. Zhu, T. Zhang, H. Lu, C. Wang, B. Xue, X. Xu, Y. Liu, Z. Cai, W. Sang, Y. Hua, J. Ma, BRD4 has dual effects on the HMGB1 and NF-kappaB signalling pathways and is a potential therapeutic target for osteoarthritis, Biochim. Biophys. Acta (BBA) - Mol. Basis Dis. 1863 (12) (2017) 3001–3015.
[28] Z. Hu, Y. Chen, L. Song, J.H.N. Yik, D.R. Haudenschild, S. Fan, Flavopiridol protects bone tissue by attenuating RANKL induced osteoclast formation, Front. Pharmacol. 9 (2018) 174.
[29] Y. Ueki, C.Y. Lin, M. Senoo, T. Ebihara, N. Agata, M. Onji, Y. Saheki, T. Kawai, P.M. Mukherjee, E. Reichenberger, B.R. Olsen, Increased myeloid cell responses to M-CSF and RANKL cause bone loss and inflammation in SH3BP2 "cherubism" mice, Cell 128 (1) (2007) 71–83.
[30] Y. Ikebuchi, S. Aoki, M. Honma, M. Hayashi, Y. Sugamori, M. Khan, Y. Kariya, G. Kato, Y. Tabata, J.M. Penninger, N. Udagawa, K. Aoki, H. Suzuki, Coupling of bone resorption and formation by RANKL reverse signalling, Nature 561 (7722) (2018) 195–200.
[31] S. Qiao, Q. Luo, Y. Zhao, X.C. Zhang, Y. Huang, Structural basis for lipopolysaccharide insertion in the bacterial outer membrane, Nature 511 (7507) (2014) 108–111.
[32] S. Wijekoon, E.C. Bwalya, J. Fang, S. Kim, K. Hosoya, M. Okumura, Chronological differential effects of pro-inflammatory cytokines on RANKL-induced osteoclast differentiation of canine bone marrow-derived macrophages, J. Vet. Med. Sci. 79 (12) (2017) 2030–2035.
[33] X. Zhu, J. Gao, P.Y. Ng, A. Qin, J.H. Steer, N.J. Pavlos, M.H. Zheng, Y. Dong, T.S. Cheng, Alexidine dihydrochioride attenuates osteoclast formation and bone resorption and protects against LPS-induced osteolysis, J. Bone Miner. Res. Off. J. Am. Soc. Bone Miner. Res. 31 (3) (2016) 560–572.
[34] L.C. Franco, F. Morales, S. Boffo, A. Giordano, CDK9: a key player in cancer and other diseases, J. Cell. Biochem. 119 (2) (2018) 1273–1284.